IMAGE DENOISING BY ADAPTIVE WAVELET THRESHOLDING WITH GENERALIZED GAUSSIAN DISTRIBUTION USING MODIFIED BAYESSHRINK THRESHOLDING ALGORITHM

[1] Pragati Sahu, [2] Shailesh Khaparkar, [3] Ritesh Beohar, [4] Pankaj Sahu
[1]Research Scholar, [2] H.O.D & Associate Professor, [3]Assistant Professor, [4]Assistant Professor
M.Tech. Communication Systems, Dept. of ECE, GGITS, Jabalpur

ABSTRACT: Visual information transmitted in the form of digital images is becoming a major method of communication in the modern age, but the image obtained after transmission is often corrupted with noise. The received image needs processing before it can be used in applications. Image denoising involves the manipulation of the image data to produce a visually high quality image. Hence, it is necessary to have knowledge about the noise present in the image so as to select the appropriate denoising algorithm. The wavelet based approach finds applications in denoising images corrupted with Gaussian noise. In this work a new image denoising algorithm by using a non-parametric statistical model of wavelet coefficients, in which 3 thresholding levels are defined for improvement of PSNR and BER performance.

KEYWORDS: AWGN, Image Denoising, Noise, Filtering, DWT, threshold, PSNR, BER.

I. INTRODUCTION

A very large portion of digital image processing is dedicated to image restoration. It includes research in algorithm development and routine goal oriented image processing. Image restoration is the removal or reduction of degradations that are incurred while the image is being obtained. Degradation comes from blurring as well as noise due to electronic and photometric sources.[2] Blurring is a form of bandwidth reduction of the image caused by the imperfect image formation process such as relative motion between the camera and the original scene or by an optical system that is out of focus. When aerial photographs are produced for remote sensing purposes, blurs are introduced by atmospheric turbulence, aberrations in the optical system and relative motion between camera and ground. In addition to these blurring effects, the recorded image is corrupted by noises too. A noise is introduced in the transmission medium due to a noisy channel, errors during the measurement process and during quantization of the data for digital storage. Each element in the imaging chain such as lenses, film, digitizer, etc. contributes to the degradation [3].

Image denoising is often used in the field of photography or publishing where an image was somehow degraded but needed to be improved before it can be printed. For this type of application we need to know something about the degradation process in order to develop a model for it. When we have a model for the degradation process, the inverse process can be applied to the image to restore it back to the original form. This type of image restoration is often used in space exploration to help eliminate artifacts generated by mechanical jitter in a spacecraft or to compensate for distortion in the optical system of a telescope [4]. Image denoising finds applications in fields such as astronomy where the resolution limitations are severe, in medical imaging where the physical requirements for high quality imaging are needed for analyzing images of unique events, and in forensic science where potentially useful photographic evidence is sometimes of extremely bad quality. Let us now consider the representation of a digital image. A 2-dimensional digital image can be represented as a 2-dimensional array of data $s(x,y)$, where (x,y) represent the pixel location. The pixel value corresponds to the brightness of the image at location (x,y). Some of the most frequently used image types are binary, gray-scale and color. Binary images are the simplest type of images and can take only two discrete values, black and white. Black is represented with the value „0" while white with „1". Note that a binary image is generally created from a gray-scale image. A binary image finds applications in computer vision areas where the general shape or outline information of the image is needed. They are also referred to as 1 bit/pixel images [5].Gray-scale images are known as monochrome or one-color images. The images used for experimentation purposes in this thesis are all gray-scale images. They contain no color information. They represent the brightness of the image. This image contains 8 bits/pixel data, which means it can have up to 256 (0-255) different brightness levels.

II. DISCRETE WAVELET TRANSFORM (DWT) BASED DENOISING APPROACH

Wavelets are mathematical functions that analyze data according to scale or Resolution. They aid in studying a signal in different windows or at different resolutions. For instance, if the signal is viewed in a large window, gross features can be noticed, but if viewed in a small window, only small features can be noticed. Wavelets provide some advantages over Fourier transforms. For example, they do a good job in approximating signals with sharp spikes or signals having discontinuities. Wavelets can also model speech, music, video and non-stationary stochastic signals. Wavelets can be used in applications such as image compression, turbulence, human vision, radar, earthquake prediction, etc. The term "wavelets" is used to refer to a set of Ortho-normal basis functions generated by dilation and translation of scaling function φ and a mother wavelet ψ. The finite scale multi resolution representation of a discrete function can be called as a discrete wavelet transform. DWT is a fast linear operation on a data vector, whose length is an integer power of 2. This transform is invertible and orthogonal, where the inverse transform expressed as a matrix is the transpose of the transform matrix. The wavelet basis or function, unlike sine and cosines as in Fourier transform, is quite localized in space. But similar to sine and cosines, individual wavelet functions are localized in frequency. The Ortho-normal basis or wavelet basis is defined as:

$$\varphi_{(j,k)}(x) = 2^{\frac{j}{2}}\varphi(2^j x - k)$$

The scaling function is given as:

$$\emptyset_{(j,k)}(x) = 2^{\frac{j}{2}}\varphi(2^j x - k)$$

Where ψ is called the wavelet function and j and k are integers that scale and dilate the wavelet function. The factor „j" is known as the scale index, which indicates the wavelet"s width. The location index k provides the position. The wavelet function is dilated by powers of two and is translated by the integer k. In terms of the wavelet coefficients, the wavelet equation is

$$\varphi(x) = \sum_{k}^{N-1} gk\sqrt{2\emptyset(2x-k)}$$

Where g0, g1, g2,…. are high pass wavelet coefficients. Writing the scaling equation in terms of the scaling coefficients as given below, we get

$$\emptyset(x) = \sum_{k}^{N-1} hk\sqrt{2\emptyset(2x-k)}$$

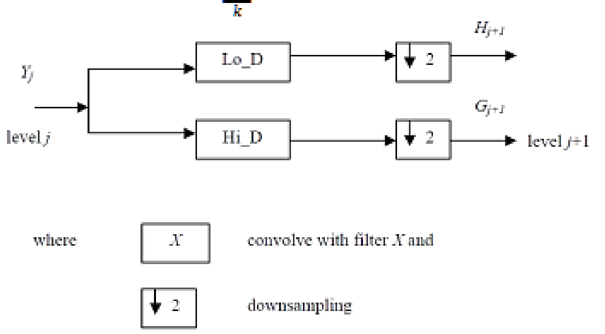

Figure 1: 1-Dimensional DWT - Decomposition step

DWT is the multi resolution description of an image. The decoding can be processed sequentially from a low resolution to the higher resolution. DWT splits the signal into high and low frequency parts. The high frequency part contains information about the edge components, while the low frequency part is split again into high and low frequency parts. The high frequency components are usually used for watermarking since the human eye is less sensitive to changes in edges. In two dimensional applications, for each level of decomposition, we first perform the DWT in the vertical direction, followed by the DWT in the horizontal direction. After the first level of decomposition, there are 4 sub-bands: LL1, LH1, HL1, and HH1. For each successive level of decomposition, the LL Sub-band of the previous level is used as the input. To perform second level decomposition, the DWT is applied to LL1 band which decomposes the LL1 band into the four sub- bands LL2, LH2, HL2, and HH2.

To perform third level decomposition, the DWT is applied to LL2 band which decompose this band into the four sub-bands – LL3, LH3, HL3, HH3. This results in 10 sub-bands per component. LH1, HL1, and HH1 contain the highest frequency bands present in the image tile, while LL3 contains the lowest frequency band.

DWT is currently used in a wide variety of signal processing applications, such as in audio and video compression, removal of noise in audio, and the simulation of wireless antenna distribution.

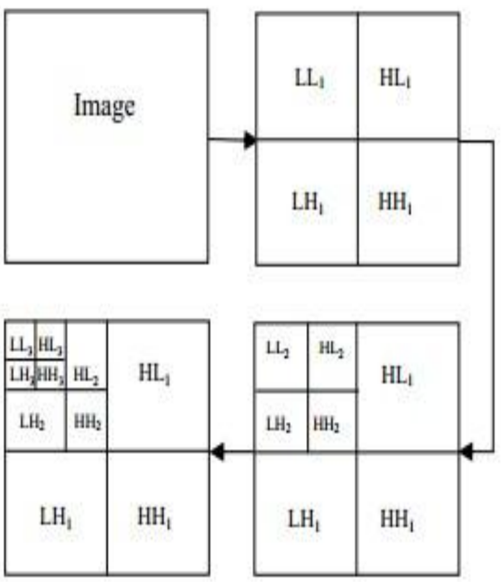

Figure 2: 3 Levels Discrete Wavelet Decomposition

Wavelets have their energy concentrated in time and are well suited for the analysis of transient, time-varying signals. Since most of the real life signals encountered are time varying in nature, the Wavelet Transform suits many applications very well. As mentioned earlier, the wavelet equation produces different wavelet families like Daubechies, Haar, Coiflets, etc.

Table 1: Wavelet Families and Their Properties

III. Wavelet Thresholding

The term wavelet thresholding is explained as decomposition of the data or the image into wavelet coefficients, comparing the detail coefficients with a given threshold value, and shrinking these coefficients close to zero to take away the effect of noise in the data. The image is reconstructed from the modified coefficients. This process is also known as the inverse discrete wavelet transform. During thresholding, a wavelet coefficient is compared with a given threshold and is set to zero if its magnitude is less than the threshold; otherwise, it is retained or modified depending on the threshold rule. Thresholding distinguishes between the coefficients due to noise and the ones consisting of important signal information.

The choice of a threshold is an important point of interest. It plays a major role in the removal of noise in images because denoising most frequently produces smoothed images, reducing the sharpness of the image. Care should be taken so as to preserve the edges of the denoised image. There exist various methods for wavelet thresholding, which rely on the choice of a threshold value. Some typically used methods for image noise removal include VisuShrink, SureShrink and BayesShrink. Prior to the discussion of these methods, it is necessary to know about the two general categories of thresholding. They are hard- thresholding and soft-thresholding types.

IV. PROPOSED DENOISING APPROACH

In this work an image denoising approach through Adaptive Wavelet Thresholding with Generalized Gaussian distribution using Modified BayesShrink Thresholding Algorithm has been proposed. This approach can be formally described as Bayesian. The formulation is based upon the empirical consideration which is that the wavelet coefficients of an image subband can be summarized adequately by a (GGD) Generalized Gaussian distribution. Also the average MSE in a subband can be anticipated by the corresponding Bayesian squared error risk with the GGD as the prior applied to each in an iid fashion. That is, a sum is approximated by an integral. The aim is to derive a new soft-threshold method which reduces the Bayesian risk, & thus the proposed algorithm is called BayesShrink.

This proposed Bayesian risk diminution is reliant on subband. The noise is AWGN & the signal is GDD, through the numerical computation an optimal threshold for soft-thresholding can be derived as; $T_B = \sigma^2/\sigma_X$ (where σ^2 is the noise variance and σ_X^2 is the signal variance). This threshold provides a risk which is in the range of 5% of the minimized risk over a large range of parameters in the generalized Gaussian distributed family. In order to devise this threshold data-driven, σ_X and σ are estimated from discerned data, one set for each subband.

The advantages of this method is that not only denoising is achieved, but at the same time compression is also done, & the non-zero thresholded wavelet coefficients requires quantization. Uniform quantizer and centroid reproduction is used on the GGD. The design parameters of the coder, such as the number of quantization levels and bin widths, are decided based on a guidelines derived from Rissanen's Minimum Description Length (MDL) principle [20].

Proposed Algorithm

1. Read the test image (original).
2. Resize the test image and convert it into Gray scale image. The images taken for rectification have a lot of variation in their sizes and hence cannot be compared on the same basis. For large sized images, the computation time for denoising is found to be more difficult and if the image size is taken smaller.
3. Noise of desired level is mixed to the test images. In this work AWGN is added for generation of noisy image. Main feature of this noise, it is independent of the image on which it is going to be applied. The pixel value altered by the additive Gaussian noise can be shown as:
$J(k,l) = x(k,l) + n$
Where n is the noise, $n \sim N(0,v)$, being distributed normally with variance v.
4. Make the noisy image to undergo discrete wavelet transform, DWT.
5. After the noisy image is decomposed into approximation and detail coefficients using wavelet transform, it is made to undergo our proposed modified thresholding rules having various threshold values. **Modified BayesShrink Thresholding** is an Adaptive Threshold for BayesShrink is the thresholding function which is modified & extended upto three different levels. By putting the derivative of risk to zero with respect to the optimal threshold is found to be:
$$T_h^*(\sigma_x, 2) = \begin{cases} 0, & if\ \sigma_x > \sigma \\ \infty, & if\ \sigma_x < \sigma \\ anything, & if\ \sigma_x = \sigma. \end{cases}$$
With the associated risk
$$r_h(T_h^*) = \begin{cases} \sigma^2, & if\ \sigma_x > \sigma \\ \sigma_x^2, & if\ \sigma_x \le \sigma. \end{cases}$$
The soft-thresholding rule is preferred than the hard-thresholding for the following reasons;
   - Soft-thresholding achieves optima in minimax rate for a large range.
   - For the Generalized Gaussian prior taken in this proposed work, the optimal soft-thresholding estimator has a minimum risk as compared to the optimal hard-thresholding estimator.
   - Soft-thresholding gives more visually gratifying images than hard-thresholding due to the fact that hard-thresholding is discontinuous and outputs sudden changes in the reconstructed image, & especially when the noise energy is significant.
6. After the decomposition, the coefficients are thresholded using the above mentioned threshold values with each of the thresholding technique, the denoised image is reconstructed using inverse wavelet transform IDWT.
7. Calculate the various standard performance parameters like MSE, PSNR, MAE & SSIM which are calculated for all the standard images with their noisy and denoised images.

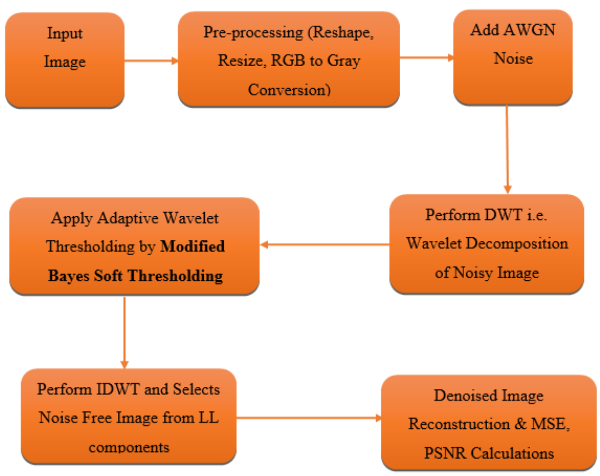

Figure 3: Flowchart of Proposed Image Denoising Method

V. RESULTS & DISCUSSIONS

In simulation we have done the simulations with different wavelets 'Haar', 'Daubechies' and 'Symlet', using soft wavelet thresholding, hard wavelet thresholding & Modified Bayes soft wavelet thresholding.

V.1 Test Image Lena & Proposed Denoising Method

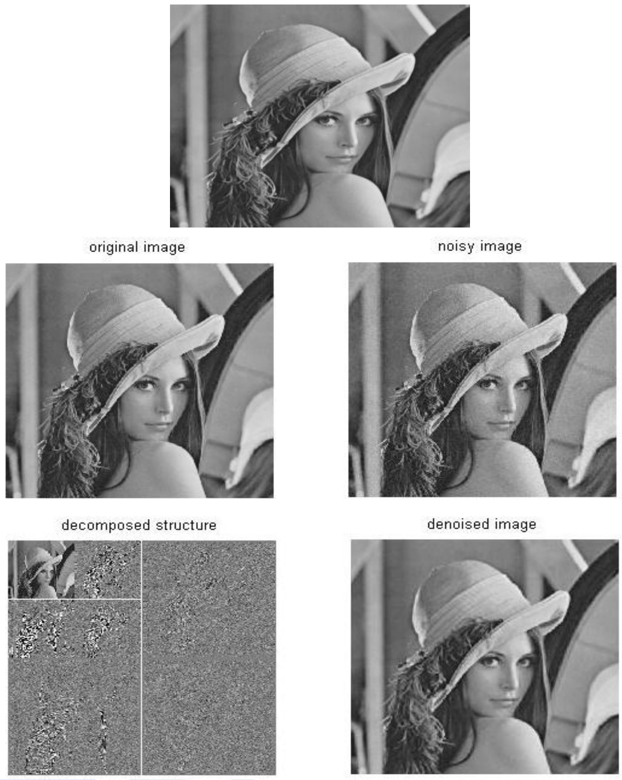

Figure 4: Denoising by Proposed Algorithm of Test Image 'Lena'

V.2 Simulation Results Summary of Proposed Work (Lena.jpg)

Noise Variance σ (dB)	Before Denoising		Soft Wavelet Thresholding		Hard Wavelet Thresholding		Modified Bayes Thresholding	
	MSE	PSNR	MSE	PSNR	MSE	PSNR	MSE	PSNR
12	143.42	26.56	90.61	28.56	59.49	30.39	**36.49**	**32.50**
14	196.11	25.21	97.51	28.24	66.87	29.88	**42.53**	**31.84**
16	256.44	24.04	106.03	27.88	75.84	29.33	**48.97**	**31.23**
18	323.15	23.04	113.02	27.60	82.66	28.96	**54.97**	**30.73**
20	398.41	22.13	119.41	27.36	90.25	28.58	**62.62**	**30.17**
22	477.63	21.34	125.18	27.16	97.91	28.22	**67.08**	**29.86**
24	568.56	20.58	131.35	26.95	105.17	27.91	**72.37**	**29.53**
26	666.90	19.89	138.72	26.71	113.44	27.58	**78.20**	**29.20**
28	770.12	19.27	143.77	26.55	121.38	27.29	**84.32**	**28.87**
30	874.75	18.71	149.74	26.38	129.62	27.00	**88.61**	**28.65**

Table 2: Test Image Lena Simulation Results

Table 2 shows overall average improvement in MSE is 47% & 32% with soft & hard wavelet thresholding respectively. Overall average improvement in PSNR is 2.92 dB & 1.74 dB with soft & hard wavelet thresholding respectively.

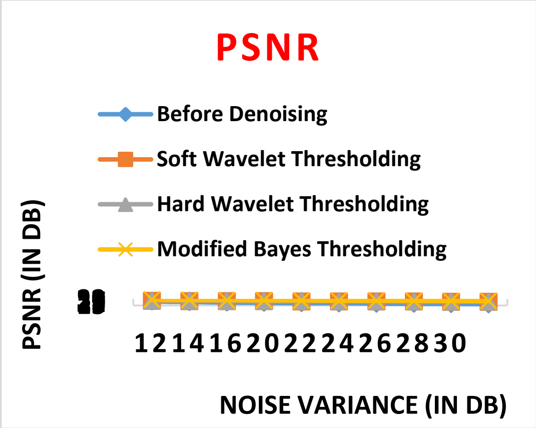

Figure 5: Graph for PSNR comparison for simulation results (Table 2)

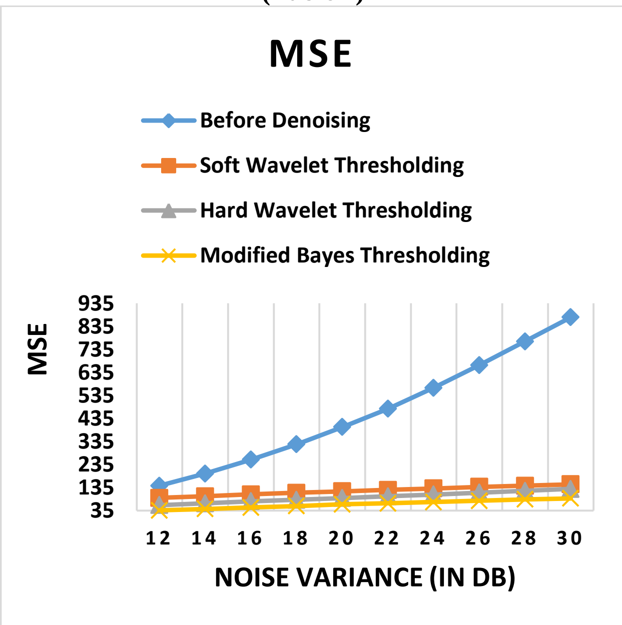

Figure 6: Graph for MSE comparison for simulation results (Table 2)

V.3 Results Comparison (Lena Image)

Noise Variance σ (dB)	Improved Threshold Base Paper [1]		Modified Bayes Thresholding	
	MSE	**PSNR**	**MSE**	**PSNR**
12	44.93	31.61	**36.49**	**32.50**
14	52.07	30.96	**42.53**	**31.84**
16	58.20	30.48	**48.97**	**31.23**
18	65.27	29.98	**54.97**	**30.73**
20	72.08	29.55	**62.62**	**30.17**
22	78.98	29.16	**67.08**	**29.86**
24	86.20	28.78	**72.37**	**29.53**
26	94.21	28.39	**78.20**	**29.20**
28	102.24	28.03	**84.32**	**28.87**
30	109.49	27.74	**88.61**	**28.65**

Table 3: Test Image Lena Simulation Results Comparison

Table 3 shows the comparison of simulation results of our proposed Modified Bayes Thresholding with the base paper [1]. From the above table it can be clearly seen that the MSE & PSNR performance of this proposed Modified Bayes Thresholding is better for all values of Noise Variance (σ). Overall average improvement in MSE is 16% and PSNR is 2.6% from the base paper [1].

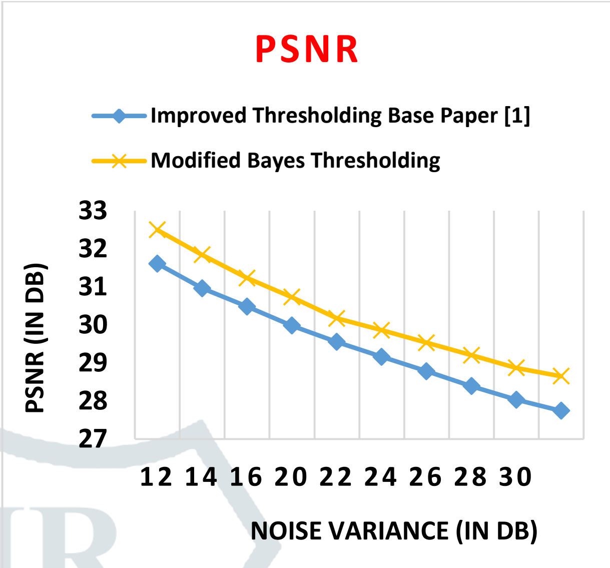

Figure 7: Graph for PSNR comparison for simulation results (Table 3)

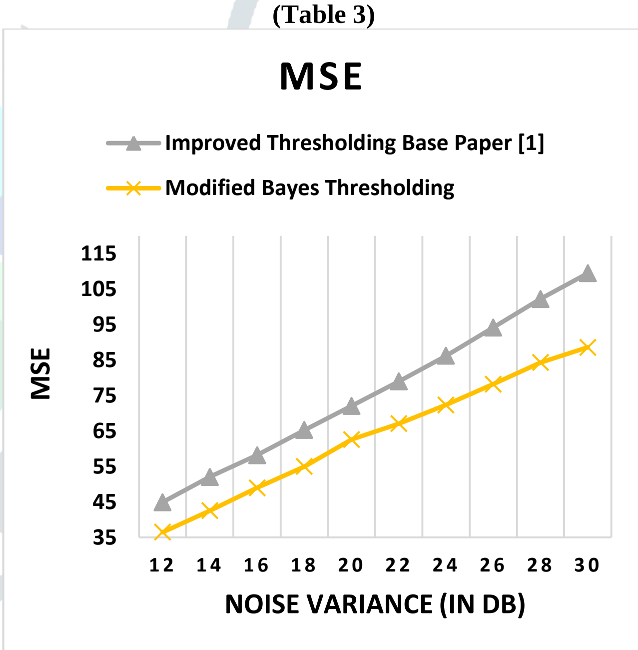

Figure 8: Graph for MSE comparison for simulation results (Table 3)

VI. CONCLUSION

In this paper image denoising techniques for the AWGN corrupted has been given. In this work an image denoising approach through Adaptive Wavelet Thresholding with Generalized Gaussian distribution using Modified BayesShrink Thresholding Algorithm has been proposed. The proposed Modified Bayes Thresholding is better for all values of Noise Variance (σ) as compared to existing thresholding methods soft & hard wavelet thresholding. Overall average improvement in MSE is 47% & 32% with soft & hard wavelet thresholding respectively. Overall average improvement in PSNR is 2.92 dB & 1.74 dB with soft & hard wavelet thresholding respectively. Also this proposed Modified Bayes Thresholding is better for all values of Noise Variance (σ). Overall average improvement in MSE is 16% and PSNR is 2.6% from the base paper [1].

REFERENCES

[1] Liqiang Shi, "An Improved Image Denoising Algorithm", Seventh IEEE International Conference on Measuring Technology and Mechatronics Automation, 2015.

[2] H. Sadreazami et-al, "Contourlet Domain Image Denoising based on the Bessel k-form Distribution", IEEE 28th Canadian Conference on Electrical and Computer Engineering Halifax, Canada, May 3-6, 2015.

[3] Cuong Cao Pham et-al, "Efficient image sharpening and denoising using adaptive guided image filtering", Published in IEEE, IET Image Processing Magazine, Pp. 71 – 79, 2015.

[4] Wangmeng Zuo et-al, "Gradient Histogram Estimation and Preservation for Texture Enhanced Image Denoising", IEEE Transactions on Image Processing, Volume 23, Nn. 6, JUNE 2014.

[5] Vikas Gupta et-al, "Image Denoising using Wavelet Transform method", Tenth IEEE International Conference on Wireless and Optical Communications Networks (WOCN), Pp 1-4, 2013.

[6] Fuqing Jia et-al, "Image Denoising Using Hyper-Laplacian Priors and Gradient Histogram Preservation Model", 12th IEEE International Conference on Signal Processing (ICSP), 2014.

[7] Ajay Boyat et-al, "Image Denoising using Wavelet Transform and Median Filtering", Nirma University IEEE International Conference on Engineering (NUiCONE), 2013.

[8] Paras Jain & Vipin Tyagi, "Spatial and frequency domain filters for restoration of noisy images", IETE Journal of Education, 54(2), 108-116, 2013.

[9] Maggioni, M., Katkovnik, V., Egiazarian, K., Foi, "A.: Nonlocal transform-domain filter for volumetric data denoising and reconstruction", IEEE Transaction on Image Processing, 22(1), 119–133, 2013.

[10] Silva, R.D., Minetto, R., Schwartz, W.R., Pedrini, H.: Adaptive edge-preserving image denoising using wavelet transforms. Pattern Analysis and Applications. Springer, Berlin doi:10.1007/s10044-012-0266-x, 2012.

[11] Zhang, Y., Li, C., Jia, J, "Image denoising using an improved bivariate threshold function in tetrolet domain", 2013.

[12] Dai, L., Zhang, Y., Li, Y.: Image denoising using BM3D combining tetrolet prefiltering. Inf. Technol. J. 12(10), 1995–2001, 2013.

[13] He, K., Sun, J., Tang, X.: Guided image filtering. In: Proceedings European Conference on Computer Vision, pp. 1–14, 2010.

[14] Porikli, F, "Constant time O(1) bilateral filtering", In Proceeding IEEE Conference on Computer Vision and Pattern Recognition, Anchorage, pp. 1–8, 2008.

[15] Yang, Q., Tan, K.H., Ahuja, N, "Real-time O(1) bilateral filtering", In Proceedings IEEE Conference on Computer Vision and Pattern Recognition, Miami, pp. 557–564, 2009.

[16] Farbman, Z., Fattal, R., Lischinski, D., Szeliski, "R.: Edge-preserving decompositions for multi-scale tone and detail manipulation", ACM Transactions on Graphics 27(3), 1–10, 2008.

[17] Paris, S., Durand, F, "A fast approximation of the bilateral filter using signal processing approach", In the Proceeding of European Conference on Computer Vision, pp. 568–580, 2006.

[18] Gonzalez, R.C., Woods, R.E.: Digital image processing, 3rd edn. Prentice-Hall, Upper Saddle River, 2008.

[19] Blu, T., Luisier, F, "The SURE-LET approach to image denoising", IEEE Transaction Image Processing, 16(11), 2778–2786, 2007.

[20] Paris, S., Durand, F.: A fast approximation of the bilateral filter using signal processing approach. In: Proceeding European Conference on Computer Vision, pp. 568–580, 2006.

[21] Dabov, K., Foi, A., Katkovnik, V., Egiazarian, K.: Image denoising with block-matching and 3D filtering. In: SPIE electronic imaging: algorithms and systems, vol. 6064, pp. 606414-1–606414-12, 2006.

[22] Yuan, X., Buckles, B.: Subband noise estimation for adaptive wavelet shrinkage. In: Proceeding 17th International Conference on Pattern Recognition, vol. 4, pp 885–888, 2004.

[23] Elad, M.: On the origin of the bilateral filter and ways to improve it. IEEE Transaction Image Processing, 11(10), 1141–1151, 2002.

[24] Sendur, L., Selesnick, I.W.: Bivariate shrinkage functions for wavelet-based denoising exploiting interscale dependency. IEEE Trans. Signal Process. 50(11), 2744–2756, 2002.

[25] Chang, S., Yu, B., Vetterli, M.: Spatially adaptive wavelet thresholding based on context modeling for image denoising. IEEE Trans. Image Process. 9(9), 1522–1531, 2000.